0.52, (2 H, m, CHCH). Carbon NMR (neat): δ -4.88 (d), -3.25 (q), 0.52 (t). MS: m/e (% relative intensity) 99 (87), 73 (100), 73 (100), 71 (29), 59 (78), 55 (10), 45 (30), 43 (52).

(E)- and (Z)-1-propenyltrimethylsilane (3 and 4, respectively) were synthesized by the method of Seyferth and Vaughn.[20] Proton NMR and IR data were identical with those previously reported. Carbon NMR of 3 (neat): δ -2.02 (q), 21.59 (q), 130.84 (d), 140.72 (d). MS: m/e (% relative intensity) 114 (11), 100 (10), 99 (97), 73 (85), 59 (100), 55 (12), 45 (12), 43 (59), 41 (51). Carbon NMR of 4 (neat): δ -0.65 (q), 18.14 (q), 129.28 (q), 142.09 (d). The mass spectrum of 4 was virtually identical with that of 3.

Allyltrimethylsilane (2) was purchased from Aldrich Chemical Co.

Kinetics Experiments. The thermal decomposition of 1 was carried out in a well-conditioned, spherical quartz reaction vessel of 250-mL capacity which was housed in an insulated 20-L stainless steel beaker containing stirred molten salt (eutectic mixture 40% $NaNO_2$, 7% $NaNO_3$, and 53% KNO_3). The bath temperature was maintained constant to +0.1 °C by a Thermotrol proportional controller (230 V), Model 1083 A (GCA Precision Scientific) with a Model 1153 platinum resistance temperature detector (GCA). Heat was provided by a stainless steel mineral insulated heating element from Chromalox Industrial Products.

Temperature was measured with a Chromel-Alumel thermocouple (Type K) in coordination with a Leeds and Northrup K-2 potentiometer. The thermocouple was immersed in a well which was placed in the center of the salt bath. Temperatures measured from the thermocouple were calibrated with a Brooklyn thermometer (range 298-355 °C). Vapors of the cyclopropylsilane were introduced into the pyrolysis vessel by expansion from a reservoir in the contiguous vacuum line. The starting sample pressure of each kinetic run was measured by a Model PDR-C-2 pressure gauge (MKS Instrument Co.) and a Model 227AHS-A-100 Baratron (MKS).

In a typical kinetic pyrolysis run the pyrolysate was sampled six times into a gas sampling bulb held at liquid-nitrogen temperature by removing an aliquot (approximately 1 torr) of the reaction mixture via expansion into a small section of the vacuum line. Starting pressure of 1 in each experiment was approximately 15 torr. Each point in a rate constant was an average of at least two GC runs. Each rate constant plot contained six points, and all reported rate constants and activation parameters were derived by a least-squared analysis of the data where each such analysis yielded a correlation coefficient of at least 0.999. Reaction of 1 was monitored chromatographically to approximately 50% decomposition, depending on temperature, and was first-order.

The role of surface effects on the course of the isomerization is minimal as suggested by a comparison of rate constants obtained in packed and unpacked reaction vessels at 416.8 °C. With a 12-fold increase in the surface to volume ratio, the change in the rate constant for decomposition was <5%. Pyrolysis of each of the reaction products, 2, 3, and 4, under conditions where 1 decomposed, indicated no secondary reaction. Predetermined response factors were measured with cyclohexane as an internal standard.

The kinetics apparatus and techniques utilized in this work were modeled on the design of Prof. H. M. Frey (Univerisity of Reading, U.K.).

Acknowledgment. We gratefully acknowledge the Robert A. Welch Foundation and the NTSU Faculty Research Fund for financial support of this work. We thank Professor W. R. Dolbier, Jr., for advice on the construction of a thermostated salt bath and Professor H. M. Frey for a stimulating introduction to the methods of gas kinetics.

Registry No. 1, 930-40-5; 2, 762-72-1; 3, 4964-03-8; 4, 4964-02-7.

(20) Seyferth, D.; L. G. *J. Organomet. Chem.* **1963**, *35*, 138-152.

Theoretical Study of Silanethione ($H_2Si{=}S$) in the Ground, Excited, and Protonated States: Comparison with Silanone ($H_2Si{=}O$)

Takako Kudo and Shigeru Nagase*

Department of Chemistry, Faculty of Education, Yokohama National University, Yokohama 240, Japan

Received September 11, 1985

To extend knowledge of silicon–sulfur double bonds, several properties of $H_2Si{=}S$ were investigated and compared with those of $H_2Si{=}O$ and $H_2C{=}O$, by means of ab initio calculations including polarization functions and electron correlation. $H_2Si{=}S$ is found to be kinetically stable enough to its unimolecular destructions such as $H_2Si{=}S \rightarrow H_2 + SiS$, $H_2Si{=}S \rightarrow H + HSiS$, and $H_2Si{=}S \rightarrow HSiSH$, as in the cases of $H_2Si{=}O$ and $H_2C{=}O$. Furthermore, it is found that $H_2Si{=}S$ is thermodynamically stable compared with $H_2Si{=}O$. Through these comparisons, it is emphasized that silicon is less reluctant to form double bonds with sulfur than with oxygen. The singlet–triplet energy differences in $H_2Si{=}S$ and $H_2Si{=}O$ are calculated to be considerably smaller than that in $H_2C{=}O$. In the protonated states, the S-protonated singlet species H_2SiSH^+ is the most stable, and it is separated by sizable barriers from its isomers H_3SiS^+ and $HSiSH_2^+$, as are H_2SiOH^+ and H_2COH^+. Finally, the potential energy surface for the reaction of $H_2Si{=}S$ with water is calculated to investigate the reactivity toward polar reagents.

Introduction

Compounds that feature double bonding to silicon are of current interest.[1] As the silicon analogues of ethenes, silicon–carbon (silenes)[2] and silicon–silicon (disilenes)[3] doubly bonded compounds have been characterized and isolated in the last few years. In contrast, the study of the formaldehyde analogues seems to be still in the early stages.[1] Recently we have studied the thermodynamic and

(1) For recent comprehensive reviews, see: (a) Gusel'nikov, L. E.; Nametkin, N. S. *Chem. Rev.* **1979**, *79*, 529. (b) Coleman, B.; Jones, M. *Rev. Chem. Intermed.* **1981**, *4*, 297. (c) Bertrand, G.; Trinquier, G.; Mazerolles, P. *J. Organomet. Chem. Libr.* **1981**, *12*, 1. (d) Schaefer, H. F. *Acc. Chem. Res.* **1982**, *15*, 283. (e) Wiberg, N. *J. Organomet. Chem.* **1984**, *273*, 141. (f) West, R. *Science (Washington, D.C.)* **1984**, *225*, 1109. (g) Raabe, G.; Michl, J. *Chem. Rev.* **1985**, *85*, 419.

(2) Brook, A. G.; Abdesaken, F.; Gutekunst, B.; Gutekunst, G.; Kallury, R. K. *J. Chem. Soc., Chem. Commun.* **1981**, 191. Brook, A. G.; Nyburg, S. C.; Abdesaken, F.; Gutekunst, B.; Gutekunst, G.; Kallury, P. K. M. R.; Poon, Y. C.; Chang, Y.-M.; Wong-Ng, W. *J. Am. Chem. Soc.* **1982**, *104*, 5667.

(3) West, R.; Fink, M. J.; Michl, J. *Science (Washington, D.C.)* **1981**, *214*, 1343. For a current review, see ref 1f.

0276-7333/86/2305-1207$01.50/0

kinetic stability of silicon–oxygen doubly bonded compounds (silanones).[4-6] Silanones are found to be less stable and more reactive than formaldehydes. This may arise from the following: unfavorable overlapping between $p_\pi(Si)$ and $p_\pi(O)$ orbitals owing to a size difference gives a weaker π-bonding, while a large electronegativity difference between Si and O atoms causes strongly polarized Si^+–O^- bonding which results in the higher reactivity. To the extent that the view is valid, silicon–sulfur doubly bonded compounds (silanethiones) are expected to be more stable and less reactive. However, the number of experimental studies of silanethiones is fairly limited to date; only indirect evidence is at present available which suggests the transient existence of the important species.[7]

In view of the situation theoretical information is of great help for further advance in silanethione chemistry. Thus, we have undertaken the first ab initio calculations of the properties of the ground and excited states of the parent compound $H_2Si{=}S$ to extend the knowledge of silicon–sulfur double bonds. To investigate its stability and reactivity, comparisons with $H_2Si{=}O$ and $H_2C{=}O$ are made with use of results obtained at the same level of theory. Also investigated is the protonation of $H_2Si{=}S$ and $H_2Si{=}O$, because of the long-standing interest in the protonation of the carbon analogues $H_2C{=}S$[8] and $H_2C{=}O$.[8,9]

To this end, silicon–sulfur double bonds are found to be thermodynamically and kinetically more stable than silicon–oxygen double bonds. Successful schemes for the synthesis and isolation of silanethiones are expected to be soon devised.

Computational Details

Stationary points (equilibrium and transition structures) on potential energy surface were all located at the Hartree–Fock (HF) level with the split-valence 6-31G* d-polarized basis set[10] by using analytical gradient procedures. In these calculations, open-shell triplet states were treated with the spin-unrestricted Hartree-Fock (UHF) formalism. UHF wave functions do not give true spin eigenfunctions, but computed expectation values of the spin-squared operator $\langle S^2 \rangle$ were in the range of 2.007–2.014 for all triplet species considered here and they were very close to the correct value of 2.0 for pure triplets.

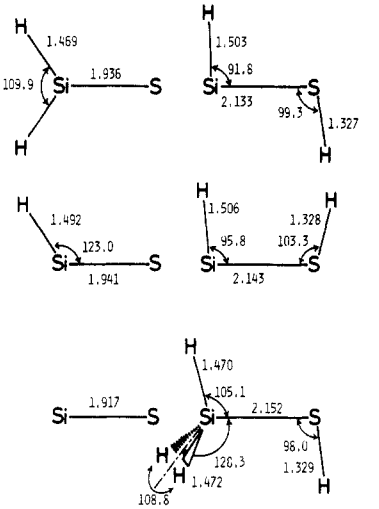

Figure 1. Equilibrium structures in angstroms and degrees calculated at the HF/6-31G* level.

Scheme I

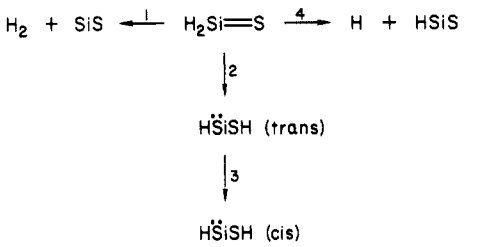

Subsequent to the full optimization of the stationary point structures, single-point calculations were carried out to obtain more reliable energies; with the larger 6-31G** basis set,[10] electron correlation was incorpolated via configuration interaction (CI) or second- and third-order Møller–Plesset perturbation (MP2 and MP3)[11] theories. In the CI calculations, all single (S) and double (D) excitations from the respective HF reference configurations were included, with the constraint that core-like orbitals (1s, 2s, and 2p for Si and S and 1s for C and O) were "frozen" (i.e, doubly occupied). The energies by the CI method were further improved with the Davidson formula[12] to allow for the unlinked cluster quadruple correction (QC), these being denoted by CI(S+D+QC). Zero-point correction (ZPC) was made with harmonic vibrational frequencies calculated at the HF/3-21G level.[13]

For $H_2Si{=}S$ only, the harmonic vibrational frequencies were calculated at the HF/6-31G* level. The zero-point energy of 11.6 kcal/mol at the HF/6-31G* level was found to differ little from that of 11.1 kcal/mol at the HF/3-21G level.

Results and Discussion

A. Closed-Shell Singlet States. The species and unimolecular reactions pertinent to the stability of $H_2Si{=}S$ are shown in Scheme I.

Structures. Figure 1 summarizes the HF/6-31G* equilibrium structures on the ground singlet potential energy surface of the H_2SiS species. At present no ex-

(4) Kudo, T.; Nagase, S. *J. Organomet. Chem.* **1983**, *253*, C23.
(5) Kudo, T.; Nagase, S. *J. Phys. Chem.* **1984**, *88*, 2833.
(6) Kudo, T.; Nagase, S. *J. Am. Chem. Soc.* **1985**, *107*, 2589.
(7) Gusel'nikov, L. E.; Sokolova, V. M.; Volnina, E. A.; Zaikin, V. G.; Nametkin, N. S.; Voronkov, M. G.; Kirpichenko, S. V.; Keiko, V. V. *J. Organomet. Chem.* **1981**, *214*, 145. Gusel'nikov, L. E.; Volkova, V. V.; Zaikin, V. G.; Tarasenko, N. A.; Tishenkov, A. A.; Nametkin, N. S.; Voronkov, M. G.; Kirpichenko, S. V. *J. Organomet. Chem.* **1981**, *215*, 9. Carlson, C. W.; West, R. *Organometallics* **1983**, *2*, 1798. Guimon, C.; Pfister-Guillouzo, G.; Lavayssiere, H.; Dousse, G.; Barrau, J.; Satge, J. *J. Organomet. Chem.* **1983**, *249*, C17. Gusel'nikov, L. E.; Volkova, V. V.; Avakyan, V. G.; Nametkin, N. S.; Voronkov, M. G.; Kirpichenko, S. V.; Suslova, E. N. *J. Organomet. Chem.* **1983**, *254*, 173. Gusel'nikov, L. E.; Volkova, V. V.; Avakyan, V. G.; Volnina, E. A.; Zaikin, V. G.; Nametkin, N. S.; Polyakova, A. A.; Tokarev, M. I. *J. Organomet. Chem.* **1984**, *271*, 191.
(8) Bernardi, F.; Csizmadia, I. G.; Schlegel, H. B.; Wolfe, S. *Can. J. Chem.* **1975**, *53*, 1144. Bernardi, F.; Csizmadia, I. G.; Mangini, A.; Schlegel, H. B.; Whangbo, M.-H.; Wolfe, S. *J. Am. Chem. Soc.* **1975**, *97*, 2209. Pau, J. K.; Ruggera, M. B.; Kim, J. K.; Caserio, M. C. *J. Am. Chem. Soc.* **1978**, *100*, 4242. Dill, J. D.; Mclafferty, F. W. *J. Am. Chem. Soc.* **1979**, *101*, 6526. Yamabe, T.; Yamashita, K.; Fukui, K.; Morokuma, K. *Chem. Phys. Lett.* **1979**, *63*, 433. Grein, F. *Can. J. Chem.* **1984**, *62*, 253. Nobes, R. H.; Bouma, W. J.; Radom, L. *J. Am. Chem. Soc.* **1984**, *106*, 2774.
(9) Schleyer, P. v. R.; Jemmis, E. D. *J. Chem. Soc., Chem. Commun.* **1978**, *190*. Dill, J. D.; Fischer, C. L.; Mclafferty, F. W. *J. Am. Chem. Soc.* **1979**, *101*, 6531. Nobes, R. H.; Radom, L.; Rodwell, W. R. *Chem. Phys. Lett.* **1980**, *74*, 269.
(10) Francl, M. M.; Pietro, W. J.; Hehre, W. J.; Binkley, J. S.; Gordon, M. S.; DeFrees, D. J.; Pople, J. A. *J. Chem. Phys.* **1982**, *77*, 3654.
(11) Pople, J. A.; Binkely, J. S.; Seeger, R. *Int. J. Quantum Chem., Quantum Chem. Symp.* **1976**, *10*, 1.
(12) Langhoff, S. R.; Davidson, E. R. *Int. J. Quantum Chem.* **1974**, *8*, 61. Davidson, E. R.; Silver, D. W. *Chem. Phys. Lett.* **1978**, *52*, 403.
(13) Gordon, M. S.; Binkley, J. S.; Pople, J. A.; Pietro, W. J.; Hehre, W. J. *J. Am. Chem. Soc.* **1982**, *104*, 2797. For comparable accuracy of HF/3-21G and HF/6-31G* vibrational frequencies, see: Pople, J. A.; Schlegel, H. B.; Krishnan, R.; DeFrees, D. J.; Binkley, J. S.; Frisch, M. J.; Whiteside, R. A.; Hout, R. F.; Hehre, W. J. *Int. J. Quantum Chem., Quantum Chem. Symp.* **1981**, *15*, 269.

perimental data are available for comparison. It may be fruitful to make comparison with the calculated values for the H_2CO[14] and H_2SiO[5] species at the same level of theory.

The equilibrium structure of $H_2Si{=}S$ is calculated to be planar with C_{2v} symmetry, as in the cases of $H_2C{=}O$ and $H_2Si{=}O$. The Si—S bond length (1.936 Å) in $H_2Si{=}S$ is 0.752 and 0.438 Å longer, respectively, than the C—O and Si—O bond lengths in $H_2C{=}O$ and $H_2Si{=}O$. However, the Si—S bond length is 0.216 Å shorter than the Si—S single bond length (2.152 Å) in $H_3Si{-}SH$, indicating that there is a certain strength in π-bonding between the Si and S atoms in $H_2Si{=}S$. The bond length shortening of 10% from $H_3Si{-}SH$ to $H_2Si{=}S$ is comparable to that of 9% from $H_3Si{-}OH$ to $H_2Si{=}O$, but it is smaller than that of 15% from $H_3C{-}OH$ to $H_2C{=}O$. The smaller shortening of silicon-containing bonds is also seen for the ethene analogues: 14% ($H_2C{=}CH_2$), 10% ($H_2Si{=}CH_2$), and 9% ($H_2Si{=}SiH_2$).

The elimination of a hydrogen atom from $H_2Si{=}S$ gives the HSiS radical. For this silicon radical, two distinct equilibrium structures with the same $^2A'$ symmetry were found, whose electronic configurations are described, respectively, as

HṠiS HSiṠ

The HṠiS and HSiṠ radicals differ greatly in their Si–S bond lengths and HSiS bond angles. The Si—S bond length (1.941 Å) in HṠiS is only 0.005 Å longer than the double bond in $H_2Si{=}S$, while the Si—S length (2.070 Å) in HSiṠ is rather close to the Si—S single bond in $H_3Si{-}SH$. In addition, the HSiS bond angle (123.0°) in HṠiS is 27.2° larger than that (95.8°) in HSiṠ. As for the relative stability, HṠiS was calculated to be 6.2 kcal/mol more stable at the MP3/6-31G**//6-31G* level than HSiṠ. Thus, only HṠiS will be considered in this paper. For the HSiO radical,[15] two minima were also found which correspond to HṠiO (SiO = 1.501 Å, SiH = 1.505 Å, and ∠HSiO = 122.8°) and HSiȮ (SiO = 1.626 Å, SiH = 1.513 Å, and ∠HSiO = 94.1°). At the MP3/6-31G**//6-31G* level, the energy difference (12.3 kcal/mol) favoring HṠiO over HSiȮ is twice as large as that favoring HṠiS over HSiṠ. For the carbon radical HCO, however, only one minimum corresponding to HĊO (CO = 1.159 Å, CH = 1.106 Å, and ∠HCO = 126.3°) was located on the potential energy surface.

The hydrogen elimination from HṠiS, HṠiO, and HĊO shortens their Si–S, Si–O, and C–O bond lengths, respectively, by 1.2, 0.9, and 3.9%. Consequently, the double bond lengths in Si=S, Si=O, and C=O are 0.019, 0.011, and 0.070 Å shorter, respectively, than those in $H_2Si{=}S$, $H_2Si{=}O$, and $H_2C{=}O$.

The divalent HS̈iSH species, the 1,2-H shifted isomers of $H_2Si{=}S$, have a planar structure in trans and cis forms. The Si–S length as well as the HSiS and HSSi angles is significantly larger in the cis form than in the trans form. These trends are also seen in HC̈OH and HS̈iOH[5] and well explained in terms of steric repulsion between the hydrogens.

Figure 2 shows the transition structures for reactions 1–3 in Scheme I. A and B are the transition structures for the

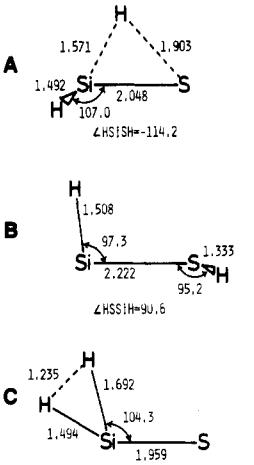

Figure 2. Transition structures in angstroms and degrees calculated at the HF/6-31G* level.

Table I. HF/6-31G* Vibrational Frequencies (cm^{-1}) of $H_2Si{=}X$ (X = S and O)[a]

symmetry and mode	$H_2Si{=}S$	$H_2Si{=}O$[b]
a_1 SiH_2 s-stretch	2424 (2153)	2433 (2160)
a_1 SiX stretch	768 (682)	1356 (1203)
a_1 SiH_2 scis.	1110 (986)	1125 (1000)
b_1 SiH_2 a-stretch	2427 (2155)	2432 (2159)
b_1 SiH_2 rock	686 (609)	787 (699)
b_2 SiH_2 wag	724 (643)	812 (721)

[a] Values in parentheses are scaled-down frequencies (see text). [b] Taken from ref 5.

1,2-hydrogen shift in $H_2Si{=}S$ to HS̈iSH (reaction 2) and trans to cis isomerization of HS̈iSH (reaction 3). Both are calculated to be nonplanar. C is the transition structure for molecular dissociation of $H_2Si{=}S$ leading to H_2 + SiS (reaction 1), which is planar. The overall features of these transition structures are very similar to those calculated previously for H_2CO and H_2SiO reactions, except that the 1,2-hydrogen shift in $H_2C{=}O$ to HC̈OH proceeds via a planar transition state.[14]

Nevertheless, it may be interesting to refer to the geometrical changes in the trans to cis isomerization of the divalent species. As Figure 2 shows, the isomerization proceeds via rotation (not via inversion). During the isomerization, no appreciable change occurs in the Si–O bond length of HS̈iOH while the Si–S and C–O lengths of HS̈iSH and HC̈OH increase by ca. 0.08 and 0.04 Å, respectively, at the transition states in which the dihedral angles are ∠HSiSH = 90.6° and ∠HCOH = 90.1°. As suggested by Goddard and Schaefer,[16] the increasings may be related to the presence of some double-bond character in the SiS and CO bonds (not in the SiO bond). At this point, it is interesting to note that the Si–S and C–O lengths of HS̈iSH and HC̈OH are 0.019 and 0.099 Å shorter, respectively, than those of H_3SiSH and H_3COH, while the Si–O length of HS̈iOH is rather comparable to that of H_3SiOH.

Vibrational Frequencies. Table I compares the harmonic vibrational frequencies of $H_2Si{=}S$ and $H_2Si{=}O$ at the HF/6-31G* level. It is now well-known that HF/6-31G* frequencies are calculated to be too high by an average of 12.6% compared with experimental (anharmonic) frequencies, but the errors are relatively constant.[17] In view of the fact, the scaled-down frequencies ($\nu_{calcd}/1.126$) are also presented in Table I. It is to be noted that the

(14) Harding, L. B.; Schlegel, H. B.; Krishnan, R.; Pople, J. A. *J. Phys. Chem.* **1980**, *84*, 3394.
(15) For recent calculations of two structures of HSiO, see: Frenking, G.; Schaefer, H. F. *J. Chem. Phys.* **1985**, *82*, 4585.
(16) Goddard, J. D.; Schaefer, H. F. *J. Chem. Phys.* **1979**, *70*, 5117.
(17) Hout, R. F.; Levi, B. A.; Hehre, W. J. *J. Comput. Chem.* **1982**, *3*, 234.

Table II. Total Energies (hartrees) of the H_2SiS Species Based on HF/6-31G* Structures

species	6-31G* HF	6-31G** HF	6-31G** CI(S+D)	6-31G** CI(S+D+QC)
$H_2Si{=}S$	−687.587 29	−687.590 37	−687.807 97	−687.829 84
H_2 + SiS	−687.568 30	−687.572 85	−687.798 47	−687.823 76
HSiSH (cis)	−687.566 04	−687.571 40	−687.788 34	−687.810 75
HSiSH (trans)	−687.569 78	−687.575 15	−687.792 52	−687.814 99
A[a]	−687.469 67	−687.475 02	−687.709 13	−687.738 19
B[a]	−687.542 02	−687.547 75	−687.762 16	−687.784 18
C[a]	−687.434 27	−687.442 54	−687.675 58	−687.703 65

[a] Transition structures in Figure 2.

Table III. Relative Energies (kcal/mol) of the H_2SiS Species Based on HF/6-31G* Structures

species	6-31G* HF	6-31G** HF	6-31G** CI(S+D)	6-31G** CI(S+D+QC)
$H_2Si{=}S$	0.0	0.0	0.0	0.0
H_2 + SiS	11.9	11.0	6.0	3.8
HSiSH (cis)	13.3	11.9	12.3	12.0
HSiSH (trans)	11.0	9.6	9.7	9.3
A[a]	73.8	72.4	62.0	57.5
B[a]	28.4	26.7	28.7	28.7
C[a]	96.0	92.8	83.1	79.2

[a] Transition structures in Figure 2.

scaled value (1203 cm^{-1}) for the Si=O stretching frequency of $H_2Si{=}O$ is in good agreement with the experimental value (1202 cm^{-1}) assigned recently by Withnall and Andrews.[18]

No experimental data on silanethiones are available for comparison. As Table I suggests, the Si=S stretching mode should be actually observed near 682 cm^{-1}. Contrary to the expectation just based on the π bond strength, the Si=S stretching frequency is predicted to be ca. 520 cm^{-1} lower than the Si=O stretching frequency. This is because the much stronger SiO σ-bonding (compared with the SiS σ-bonding) overwhelms the weaker SiO π-bonding (compared with the SiS π-bonding),[19] resulting in the greater ($\sigma + \pi$) strength of the Si=O bond than the Si=S bond.[20]

Energies. The total and relative energies of the H_2SiS species at several levels of theory are given in Tables II and III, respectively. The relative energies at the CI(S+D+QC)/6-31G**//6-31G* level are schematically summarized in Figure 3, together with the zero-point correction (ZPC) values. Since comparison of the H_2CO and H_2SiO species has already been made in our recent paper,[5] we here concentrate mainly on the similarities and differences between the H_2SiO and H_2SiS species. For this purpose, the energy profile of the H_2SiO species calculated previously[5] at the same level of theory is included in Figure 3.

As seen in Figure 3, $H_2Si{=}O$ is 2.4 kcal/mol less stable than HSiOH (at this point, note that $H_2C{=}O$ is 53.9 kcal/mol more stable than HCOH).[5] However, $H_2Si{=}S$ is now calculated to be 8.9 kcal/mol more stable than HSiSH, the relative stability of doubly bonded and divalent species being significantly reversed.

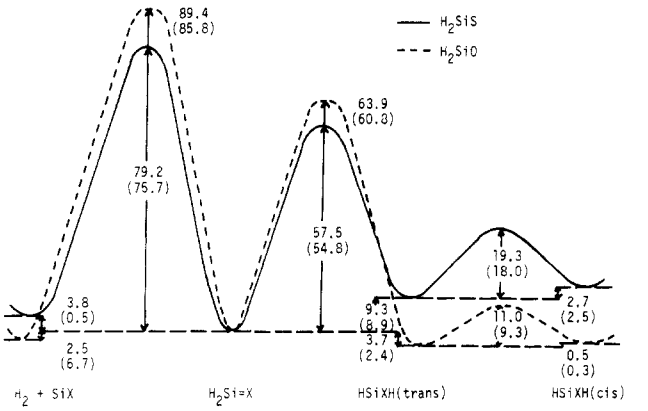

Figure 3. Schematic comparison of the energy profiles (kcal/mol) of H_2SiS (full line) and H_2SiO (dotted line) at the CI(S+D+QC)/6-31G**//6-31G* level. The zero-point corrected values are in parentheses.

Table IV. HF/6-31G* Optimized Structures for the $^3A''(n{-}\pi^*)$ and $^3A'(\pi{-}\pi^*)$ States of H_2SiX (X = S or O)

structural parameters[a]	$^3A''(n{-}\pi^*)$ H_2SiS	$^3A''(n{-}\pi^*)$ H_2SiO	$^3A'(\pi{-}\pi^*)$ H_2SiS	$^3A'(\pi{-}\pi^*)$ H_2SiO
Si-X	2.147	1.686	2.182	1.714
Si-H	1.477	1.478	1.475	1.476
∠HSiH	110.7	111.4	109.2	109.4
θ[b]	57.3	59.8	52.9	54.5

[a] Lengths in angstroms and angles in degrees. [b] Out-of-plane angles (see text).

In an attempt to assess the strength of silicon–sulfur double bonds, it is of interest to compare energies released upon the addition of H_2 to $H_2Si{=}S$, $H_2Si{=}O$, and $H_2C{=}O$. At the MP3/6-31G**/6-31G* level the hydrogenation energy of $H_2Si{=}S$ was calculated to be 31.4 kcal/mol. At the same level of theory, this value is 20.2 kcal/mol smaller than the value (51.6 kcal/mol) of $H_2Si{=}O$ and rather comparable to the value (29.6 kcal/mol) of $H_2C{=}O$. With these calculated hydrogenation energies, the π bond energies E_π(Si=S), E_π(Si=O), and E_π(C=O) are estimated, respectively, by the following equations.

$$E_\pi(\mathrm{Si{=}S}) = E(\mathrm{Si{-}H}) + E(\mathrm{S{-}H}) - E(\mathrm{H{-}H}) - 31.4$$

$$E_\pi(\mathrm{Si{=}O}) = E(\mathrm{Si{-}H}) + E(\mathrm{O{-}H}) - E(\mathrm{H{-}H}) - 51.6$$

$$E_\pi(\mathrm{C{=}O}) = E(\mathrm{C{-}H}) + E(\mathrm{O{-}H}) - E(\mathrm{H{-}H}) - 29.6$$

If one uses the values of E(H—H) = 109, E(Si—H) ≒ 90,[21] E(S—H) = 92,[22] E(O—H) = 104,[22] and E(C—H) = 98[22] kcal/mol, the π bond energies E_π(Si=S), E_π(Si=O), and E_π(C=O) would be calculated to be 42, 33, and 63 kcal/mol, respectively. This suggests that the π bond in $H_2Si{=}S$ is significantly stronger than that in $H_2Si{=}O$, though it is much weaker than that in $H_2C{=}O$.

We turn to the kinetic stability of silicon–sulfur double bonds. As Figure 3 shows, the barrier for the 1,2-H shift in $H_2Si{=}S$ to HSiSH is 54.8 kcal/mol. The more sizable barriers are present for the molecular and radical dissociations of $H_2Si{=}S$ which lead to H_2 + SiS and H + HSiS, respectively; the energies required for the former reaction is 75.7 kcal/mol, as shown in Figure 3, while the latter reaction was calculated to be 82.8 kcal/mol endothermic at the MP3/6-31G**//6-31G* level. These do suggest that $H_2Si{=}S$ itself is stable to the unimolecular destructions and is certainly the existing species. The barriers for the

(18) Withnall, R.; Andrews, L. *J. Am. Chem. Soc.* **1985**, *107*, 2567.
(19) In our recent study,[6] the $2H_2Si{=}O \rightarrow (H_2SiO)_2$ and $2H_2Si{=}S \rightarrow (H_2SiS)_2$ reactions are calculated to be 109.4 and 70.8 kcal/mol exothermic, respectively, at the MP2/6-31G*//6-31G* level. The much larger exothermicity in the dimerization of $H_2Si{=}O$ results undoubtedly from the cleavage of the weaker SiO π bonds (compared with the SiS π bonds) and the formation of the stronger SiO single bonds (compared with the SiS single bonds).
(20) In fact, the dissociation energy (128 kcal/mol) for $H_2Si{=}O \rightarrow H_2Si(^1A_1) + O(^3P)$ is calculated to be 32 kcal/mol larger at the MP3/6-31G**//6-31G* level than that (96 kcal/mol) for $H_2Si{=}S \rightarrow H_2Si(^1A_1) + S(^3P)$.
(21) Walsh, R. *Acc. Chem. Res.* **1981**, *14*, 246.
(22) Benson, S. W. *Chem. Rev.* **1978**, *78*, 23.

Table V. Net Atomic Charge Densities and Dipole Moments (D) for the Ground ($^1A_1$) and Excited ($^3A''$ and $^3A'$) States of H_2SiX (X = S or O) at the HF/6-31G//6-31G* Level**

states	atomic charge densities Si	X	H	dipole moments
		H_2SiS		
$^1A_1$(ground)	0.673	−0.416	−0.129	3.72
$^3A''(n-\pi^*)$	0.496	−0.234	−0.131	1.53
$^3A'(\pi-\pi^*)$	0.527	−0.255	−0.136	1.67
		H_2SiO		
$^1A_1$(ground)	0.998	−0.680	−0.159	4.14
$^3A''(n-\pi^*)$	0.726	−0.426	−0.150	1.77
$^3A'(\pi-\pi^*)$	0.769	−0.443	−0.163	1.76

unimolecular destructions of $H_2Si{=}S$ are calculated to be somewhat small compared with those of $H_2Si{=}O$. This reflects that the SiH bonds in $H_2Si{=}S$ are weaker than those in $H_2Si{=}O$. In fact, the energy (85.3 kcal/mol) required for the radical dissociation of $H_2Si{=}O$ was 2.5 kcal/mol larger than that of $H_2Si{=}S$ at the MP3/6-31G**//6-31G* level.

The 1,2-H-shifted isomers HS̈iSH and HS̈iOH can exist in trans and cis forms, the trans being slightly more stable than the cis, as shown in Figure 3. The barrier for the trans-to-cis isomerization via rotation of HS̈iSH is 18.0 kcal/mol while that of HS̈iOH is 9.3 kcal/mol. The former value is about twice larger than the latter value. This is explained in terms of the double bond character in the Si–S bond of HS̈iSH, as already pointed out.

B. Open-Shell Triplet States. Structures. In Table IV are summarized the structural parameters optimized at the HF/6-31G* level for the n–π^* and $\pi-\pi^*$ triplet states of H_2SiS and H_2SiO. We initially optimized the structures of these triplet states with a C_{2v} symmetry constraint. In all cases, however, the resultant optimized structures were found to be transition states for molecular deformation from the planar C_{2v} to pyramidalized C_s forms, as in the case of H_2CO.

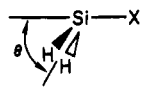

X = S or O

In the $^3A''(n-\pi^*)$ states the out-of-plane angles θ (defined as the angles between the HSiH plane and SiX axis) increase to 57.3° for H_2SiS and 59.8° for H_2SiO; at the MP3/6-31G**//6-31G*+ZPC level the pyramidalized forms of H_2SiS and H_2SiO were calculated to be 11.8 and 16.7 kcal/mol more stable, respectively, than the planar forms. In the $^3A'(\pi-\pi^*)$ states, the out-of-plane angles θ are smaller but still as large as 52.9° (H_2SiS) and 54.5° (H_2SiO).

The difference in the angles θ between the $^3A''(n-\pi^*)$ and $^3A'(\pi-\pi^*)$ states is due to the fact that the π orbitals are delocalized over the two heavy atoms while the n orbitals are strongly localized on the non-silicon atoms. In other words, a larger amount of electron transfer to silicon can take place in the $^3A'(n-\pi^*)$ states than in the $^3A'(\pi-\pi^*)$ states, as is obvious from the net atomic charge densities and dipole moments in Table V, thereby inducing sp^3 hybridization on silicon to a greater extent in the $^3A''(n-\pi^*)$ states. When comparison is made between H_2SiS and H_2SiO, H_2SiO is more pyramidalized in the $^3A''(n-\pi^*)$ and $^3A'(\pi-\pi^*)$ states than is H_2SiS. This is also explained in terms of the amount of electron transfer to silicon (see Table V), as is apparent from the fact that the strongly polarized π and π^* orbitals of H_2SiO have much smaller

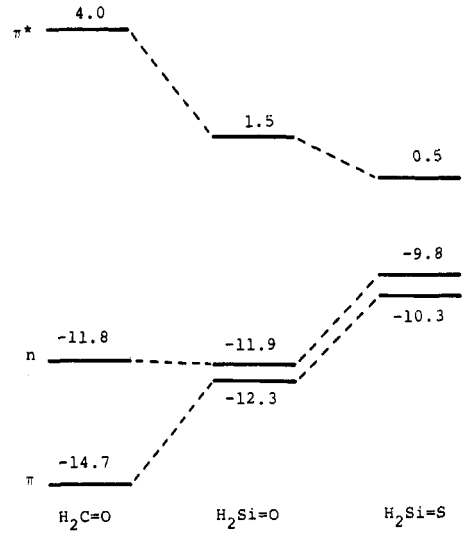

Figure 4. Frontier orbital energy energy levels (eV) of $H_2C{=}O$, $H_2Si{=}O$, and $H_2Si{=}S$ at the HF/6-31G**//6-31G* level.

Scheme II

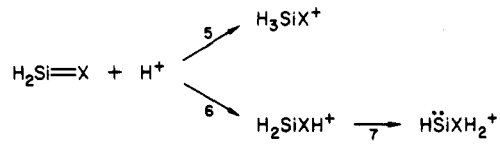

and larger electron densities around the Si atom, respectively, than those of H_2SiS.

Upon being excited to triplet states, the Si–S bond length in H_2SiS increases by 0.211 ($^3A''$) and 0.246 ($^3A'$) Å while the Si–O bond length in H_2SiO increases by 0.188 ($^3A''$) and 0.216 ($^3A'$) Å; in both the cases the increasings are larger in the $^3A'$ states than in the $^3A''$ states. All these increases are not surprising since the triplet states result from the excitation from the bonding π or nonbonding n to antibonding π^* orbitals.

Adiabatic Energy Separations. Table VI summarizes the energies of the open-shell triplet states of H_2SiS and H_2SiO, relative to the respective closed-shell singlet states. To refer to the reliability of the calculated values, we also calculated the $^3A''$ and $^3A'$ states of H_2CO because experimental data are available for the $^3A''$ state. The $^1A_1$–$^3A''$ adiabatic energy separation of 3.06 (2.97 after ZPC) eV in H_2CO calculated at the MP3/6-31G**//6-31G* level is in good agreement with the corresponding experimental value of 3.12 eV.[23] Furthermore, it is instructive to note that our MP3/6-31G**//6-31G* values for H_2SiO agree very well (to within 0.07 eV) with the values of 2.24 ($^1A_1$–$^3A''$) and 2.59 ($^1A_1$–$^3A'$) eV calculated independently by Dixon et al.[24]

As Table VI shows, $H_2Si{=}S$ and $H_2Si{=}O$ have ground singlet $^1A_1$ states, respectively, as does $H_2C{=}O$. The $^3A''(n-\pi^*)$ states of $H_2Si{=}S$ and $H_2Si{=}O$, which are the lowest excited states,[25] lie 1.75 (1.72 after ZPC) and 2.31 (2.27 after ZPC) eV, respectively, above the ground singlet $^1A_1$ states. The $^1A_1$–$^3A''$ energy separations in $H_2Si{=}S$ and $H_2Si{=}O$ are considerably smaller than that in $H_2C{=}O$. The same is also true for the $^1A_1$–$^3A'$ energy separations. These smaller energy separations are characteristic of silicon-containing compounds and easily understandable

(23) Herzberg, G. *Electronic Spectra of Polyatomic Molecules*, Van Nostrand: New York, 1966.
(24) Glinski, R. J.; Gole, J. L.; Dixon, D. A. *J. Am. Chem. Soc.* **1985**, *107*, 5891.
(25) For the calculations of the higher singlet, triplet, and Rydberg excited states at the MRD-CI level, see: Kudo, T.; Nagase, S. *Chem. Phys. Lett.*, submitted for publication.

Table VI. Singlet-Triplet Adiabatic Separation Energies (eV) in H_2SiS, H_2SiO, and H_2CO Based on HF/6-31G* Structures

	H_2SiS		H_2SiO		H_2CO	
level of theory	$^3A''$	$^3A'$	$^3A''$	$^3A'$	$^3A''$	$^3A'$
HF/6-31G*	0.94	1.16	1.05	1.32	1.95	2.89
HF/6-31G**	0.94	1.16	1.06	1.32	1.94	2.88
MP2/6-31G**	1.89	2.20	2.85	3.19	3.43	4.66
MP3/6-31G**	1.75	2.05	2.31	2.65	3.06	4.22

Table VII. Total Energies (hartrees) of the Protonated States of $H_2Si{=}S$ and $H_2Si{=}O$ Based on HF/6-31G* Structures

		6-31G**		
species	6-31G* HF	HF	MP2	MP3
H_2SiSH^+ ($^1A'$)	−687.894 20	−687.901 65	−688.107 15	−688.134 42
H_3SiS^+ ($^1A'$)	−687.776 51	−687.781 24	−687.966 04	−688.000 51
H_3SiS^+ ($^3A_1$)	−687.861 60	−687.866 32	−688.036 19	−688.068 01
$HSiSH_2^+$	−687.856 03	−687.865 00	−688.066 18	−688.098 52
D[a]	−687.761 33	−687.772 23	−688.002 21	−688.030 90
H_2SiOH^+ ($^1A'$)	−365.257 93	−365.269 07	−365.530 73	−365.542 41
H_3SiO^+ ($^1A'$)	−365.018 32	−365.023 27	−365.235 88	−365.267 52
H_3SiO^+ ($^3A_1$)	−365.145 60	−365.150 53	−365.335 28	−365.365 07
$HSiOH_2^+$ ($^1A'$)	−365.224 14	−365.238 91	−365.499 62	−365.517 86
E[a]	−365.112 92	−365.127 73	−365.411 23	−365.420 82

[a] Transition structures in Figure 6.

Table VIII. Relative Energies (kcal/mol) of Protonated States of $H_2Si{=}S$ and $H_2Si{=}O$ Based on HF/6-31G* Structures

		6-31G**			
species	6-31G* HF	HF	MP2	MP3	+ZPC
H_2SiSH^+ ($^1A'$)	0.0	0.0	0.0	0.0	0.0
H_3SiS^+ ($^1A'$)	73.9	75.6	88.5	84.0	83.4
H_3SiS^+ ($^3A_1$)	20.5	22.2	44.5	41.7	41.2
$HSiSH_2^+$	24.0	23.0	25.7	22.5	21.5
D[a]	83.4	81.2	65.9	65.0	61.7
H_2SiOH^+ ($^1A'$)	0.0	0.0	0.0	0.0	0.0
H_3SiO^+ ($^1A'$)	150.4	154.2	185.0	172.5	168.7
H_3SiO^+ ($^3A_1$)	70.5	74.4	122.6	111.3	108.4
$HSiOH_2^+$ ($^1A'$)	21.2	18.9	19.5	15.4	17.7
E[a]	91.0	88.7	75.0	76.3	73.9

[a] Transition structures in Figure 6.

from the frontier orbital energy levels shown in Figure 4. Furthermore, it is interesting to note that the energy gaps between the $^3A''(n-\pi^*)$ and $^3A'(\pi-\pi^*)$ states in $H_2Si{=}S$ and $H_2Si{=}O$ are very small (ca. 0.3 eV) compared with that in $H_2C{=}O$, because the n and π energy levels are almost degenerate in the silicon-containing compounds.

C. Protonated States. The species and reactions considered for the protonation of $H_2Si{=}X$ (X = S or O) are shown in Scheme II.

The Sites of Protonation. There are two possible sites available for the protonation of $H_2Si{=}X$ (X = S or O). Protonation on the X site (reaction 6) leads to the cation H_2SiXH^+ while protonation on the Si site (reaction 5) results in producing the cation H_3SiX^+. The HF/6-31G* optimized structures of these cations are shown in Figure 5.

The X-protonated structure H_2SiXH^+ is found to be planar with C_s symmetry. The Si–X bond length in H_2SiXH^+ is only 0.096 (X = S) and 0.063 (X = O) Å longer than that in $H_2Si{=}X$. This is because the cation results from the proton attack on the lone-pair orbitals of $H_2Si{=}X$. Interesting is the SiXH angle which may measure the direction of the lone pair orbitals (or the direction of protonation); the SiSH angle (97.7°) in H_2SiSH^+ is 34.7° smaller than the SiOH angle (132.4°) in H_2SiOH^+.

Protonation on the Si site proceeds by attacking the π orbital of $H_2Si{=}X$.[26] The Si-protonated cation H_3SiX^+

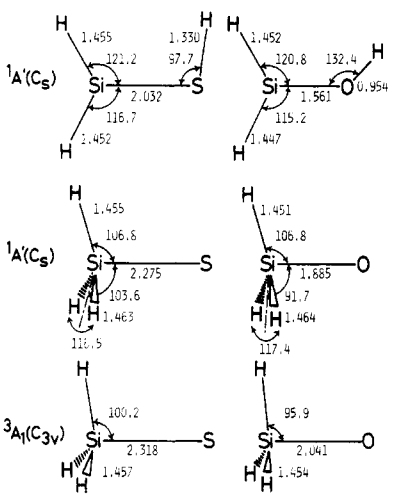

Figure 5. HF/6-31G* structures of the SiH_3S^+ and SiH_3O^+ species in angstroms and degrees.

with three equivalent hydrogen atoms has degenerate HOMO levels. According to Hund's rule the most stable should be a triplet of C_{3v} symmetry. However, Jahn–Teller distortion in a singlet state can remove the degeneracy by lowering the symmetry to C_s. For this reason, both singlet and triplet states were examined for the cation H_3SiX^+. As Figure 5 shows, the triplet cation, although optimized without symmetry constraint, is found to prefer a C_{3v} structure, in agreement with Hund's rule. As for two Jahn–Teller-distorted structures for the singlet cation, only one of them was located at the HF/6-31G* level,[27] re-

(26) One may consider that protonation on π bonding leads to a cation with bridged structures. However, no minimum corresponding to bridged structures was located at the HF/6-31G* level.

spectively, for X = S and X = O, which is just shown in Figure 5.

The total and relative energies of the cations H_2SiXH^+ ($^1A'$) and H_3SiX^+ ($^1A'$ and $^3A_1$) are given in Tables VII and VIII, respectively. In both X = S and X = O, the X-protonated cation is calculated to be much more stable at any levels of theory than the Si-protonated cation.

At the MP3/6-31G**//6-31G*+ZPC level H_2SiSH^+ ($^1A'$) is 83.4 and 41.2 kcal/mol more stable, respectively, than H_3SiS^+ ($^1A'$) and H_3SiS^+ ($^3A_1$). We managed to locate a transition state connecting H_2SiSH^+ ($^1A'$) and H_3SiS^+ ($^1A'$) at the HF/6-31G level but found that the transition state lies in energy rather below H_3SiS^+ ($^1A'$) at the higher calculational levels. This suggests that H_3SiS^+ ($^1A'$) collapses without a significant barrier to H_2SiSH^+ ($^1A'$) and that the H_3SiS^+ species is likely to exist only in a triplet state. In the protonation of $H_2Si{=}O$, H_3SiO^+ ($^1A'$) and H_3SiO^+ ($^3A_1$) are 168.7 and 108.4 kcal/mol more unstable at the MP3/6-31G**//6-31G*+ZPC level, respectively, than H_2SiOH^+ ($^1A'$). In addition, H_3SiO^+ ($^1A'$) was found to collapse to H_2SiOH^+ ($^1A'$) with no barrier, as in the case of H_3SiS^+ ($^1A'$).

The sites for the protonation of the carbon analogues $H_2C{=}X$ (X = O or S) have been extensively discussed many times over the past years.[8,9] It is now established through the long-standing controversy that H_2CXH^+ is more stable than H_3CX^+. Here, it is interesting to note that the energy difference favoring H_2SiXH^+ over H_3SiX^+ is calculated to be much larger than that favoring H_2CXH^+ over H_3CX^+.

H_2SiSH^+ vs. H_2SiOH^+. We already found that the most stable conformation of H_2SiXH^+ (X = S or O) is the fully planar structure with C_s symmetry (Figure 5). As other conformational alternatives, a nonplanar structure (**a**) and a linear Si–X–H arrangement (**b**) were investigated.

When X = S, both **a** and **b** are found to be stationary points on the potential energy surface. However, the force constant matrix analyses reveal that **a** has one negative eigenvalue while **b** has two negative eigenvalues. In other words, **b** is the maximum with respect to both molecular deformation to **a** and linear inversion at the X center, **b** being 45.7 (44.3 after ZPC) kcal/mol less stable at the MP3/6-31G**//6-31G* level than the planar C_s structure in Figure 5. On the other hand, **a** is the transition structure[28] for the rotation around the Si–X bond; the rotational barrier is calculated to be 17.5 (16.6 after ZPC) kcal/mol at the MP3/6-31G**//6-31G* level. The considerable barrier suggest a certain degree of π-bonding between the Si and S atoms in H_2SiSH^+, allowing us to describe the cation as $H_2Si{=}SH^+$. This is also supported by the fact that the Si–S stretching frequency in H_2SiSH^+ is calculated to be only 113 cm^{-1} lower than that in $H_2Si{=}S$.

When X = O, **b** is found to be the transition structure[29,30]

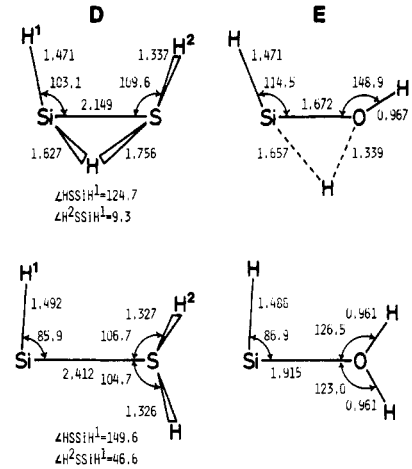

Figure 6. HF/6-31G* optimized structures of the transition states (D and E) and the products for the 1,2-H shifts in H_2SiSH^+ and H_2SiOH^+.

Table IX. Proton Affinities (kcal/mol) Calculated on HF/6-31G* Structures

level of theory	$H_2Si{=}S$	$H_2Si{=}O$	$H_2C{=}O$
HF/6-31G*	192.6	215.6	182.0
HF/6-31G**	195.4	220.6	186.6
MP2/6-31G**	193.1	209.4	180.3
MP3/6-31G**	196.1	215.7	183.2
+ZPC	190.5	208.3	174.7

for inversion at the X center and calculated to lie only 3.4 (3.1 after ZPC) kcal/mol, at the MP3/6-31G**/6-31G* level, above the planar C_s structure in Figure 5. On the other hand, **a** is found to be no longer stationary (and collapses to **b**). Therefore, a rigid rotor model was employed to evaluate approximately the rotational barrier of H_2SiOH^+. The barrier was calculated to be small (6.8 kcal/mol at the MP3/6-31G** level) even for a rigid rotation. These suggest that H_2SiOH^+ stereomutates rapidly by both inversion and rotation, and it is conformationally very flexible compared with H_2SiSH^+, H_2COH^+, and the related species.[31]

1,2-H Shifts in H_2SiSH^+ and H_2SiOH^+. Since there is a tendency for silicon to be divalent, the 1,2-H shifts (reaction 7 in Scheme II) were examined to determine the stability of the H_2SiSH^+ and H_2SiOH^+ cations.

As Figure 6 shows, the structure of the 1,2-H-shifted divalent isomer is significantly pyramidalized for $H\ddot{S}iSH_2^+$ but planar with C_s symmetry for $H\ddot{S}iOH_2^+$.[32] In a way to reach these divalent isomers via a least-motion path, the 1,2-H shift in H_2SiSH^+ prefers a nonplanar transition state (D) while that in H_2SiOH^+ proceeds via a planar transition state (E). As shown in Table VIII, the respective barriers for the 1,2-H shift are 61.7 and 73.9 kcal/mol at

(27) At the lower levels of theory, however, two Jahn–Teller-distorted structures were located.

(28) The HF/6-31G* structure has SiS = 2.081 Å, SiH = 1.456 Å, SH = 1.336 Å, ∠HSSi = 95.0° ∠HSiS = 121.2°, and ∠HSiSH = 91.5°.

(29) The HF/6-31G* structure has SiO = 1,530 Å, SiH = 1.450 Å, OH = 0.946 Å, and ∠HSiO = 118.6°.

(30) A reviewer suggests that the linearization of the internal rotation transition state is an artifact of the use of a single determinant wave function. Although at present we are unable to give a clear answer at this point, it is instructive to note that for the isovalent species H_2CNH the inversion barrier is calculated to be substantially smaller than the rotational barrier even at the MRD-CI level (Bonačič-Koutecký, V.; Persico, M. *J. Am. Chem. Soc.* **1983**, *105*, 3388). In addition, a recent paper by Cremer et al.[31] is noteworthy, in which it is found that the barriers to inversion of the related compounds H_2CYH decrease with increasing electronegativity of atom Y. This finding is in agreement with the change in the mechanism of stereomutation from H_2SiSH^+ to H_2SiOH^+.

(31) Cremer, D.; Gauss, J.; Childs, R. F.; Blackburn, C. *J. Am. Chem. Soc.* **1985**, *107*, 2435.

(32) The Walsh rule suggests a pyramidalized C_{3v} structure for the parent cations; the structure of SH_3^+ is twice more pyramidalized than that of OH_3^+, as characterized by the respective out-of-plane angles θ (θ = 0 for a planar structure) of 79.5 and 38.1° at the HF/6-31G* level. Displacement of a hydrogen by an electron-donating SiH group relaxes the degree of pyramidalization.

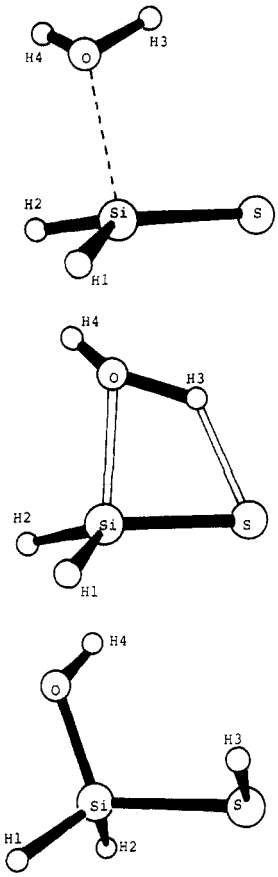

Figure 7. Ortep drawings of an intermediate compex (top), the product (bottom), and the transition state (middle) connecting them, calculated at the HF/6-31G* level for the $H_2O + H_2SiS$ reaction.

the MP3/6-31G**//6-31G*+ZPC level. This indicates that both H_2SiSH^+ and H_2SiOH^+ are kinetically stable to the 1,2-H shifts. In addition, H_2SiSH^+ and H_2SiOH^+ are calculated to be 21.5 and 17.7 kcal/mol more stable, respectively, than the 1,2-H-shifted isomers. Apparently, silicon has a much smaller tendency for divalency in cationic species than in neutral species.

Proton Affinities. Table IX compares the calculated proton affinities of $H_2Si{=}S$, $H_2Si{=}O$, and $H_2C{=}O$ at several levels of theory. The zero-point corrected MP3/6-31G**//6-31G* value of 174.7 kcal/mol for $H_2C{=}O$ agrees well with the experimental value of 171.7 kcal/mol.[33]

The proton affinities increase in the order $H_2C{=}O$ (174.7 kcal/mol) < $H_2Si{=}S$ (190.5 kcal/mol) < $H_2Si{=}O$ (208.3 kcal/mol). This is explained in terms of the predominance of the electrostatic over charge transfer interactions, because the charge separations in the double bonds increase in the order $H_2C^{+0.2}{-}O^{-0.4}$ < $H_2Si^{+0.7}{-}S^{-0.4}$ < $H_2Si^{+1.0}{-}O^{-0.7}$ (Table V) while the frontier n orbital levels rise in the order $H_2C{=}O$ (−11.8 eV) ≒ $H_2Si{=}O$ (−11.9 eV) < $H_2Si{=}S$ (−9.8 eV) (Figure 4).

D. Reactivity toward Polar Reagents. In an attempt to characterize the reactivity of silanethione toward polar reagents, we have calculated the potential energy surface for the reaction of $H_2Si{=}S$ with water as a typical example.

As Figure 7 shows, the reaction of $H_2Si{=}S$ with water initiates the formation of a two-center-like complex with maximal interaction between the oxygen and silicon atoms. The intermediate complex is transformed via a four-center-like transition state to the product $HOSiH_2SH$. The HF/6-31G* structural parameters of the complex, transition state, and product are given in Table X. It is to be noted that the overall feature of the structural changes in the $H_2Si{=}S + H_2O$ reaction is essentially the same as that calculated previously[5] in the $H_2Si{=}O + H_2O$ reaction.

As Figure 8 shows, however, the energy profile for the $H_2Si{=}S + H_2O$ reaction differs considerably from that for the $H_2Si{=}O + H_2O$ reaction. First, the $H_2Si{=}S + H_2O$ reaction is 23 kcal/mol less exothermic than the $H_2Si{=}O + H_2O$ reaction. Second, silanethione complexes water with a stabilization energy of 17.2 kcal/mol more weakly than does silanone with a stabilization energy of 21.1 kcal/mol. Third, the $H_2Si{=}S + H_2O$ complex must surmount a considerable barrier of 11.5 kcal/mol to accomplish the reaction while the $H_2Si{=}O + H_2O$ complex proceeds just across a small barrier of 4.8 kcal/mol to the silanediol product.

Table X. Structures and Total Energies Calculated for the Reaction of $H_2Si{=}S$ with H_2O

	complex	transition state	product
	Bond Distances, Bond Angles, and Dihedral Angles[a]		
SiS	1.975	2.055	2.146
SiO	2.007	1.795	1.640
SiH1	1.469	1.465	1.464
SiH2	1.475	1.471	1.470
SH3	2.938	1.726	1.329
OH3	0.958	1.215	
OH4	0.954	0.954	0.947
SSiO	103.7	87.6	112.9
SSiH1	123.6	121.5	111.1
SSiH2	123.5	120.9	103.0
SiSH3	56.1	62.7	98.2
SiOH3	106.9	80.0	
SiOH4	115.9	120.2	119.2
H1SiSO	−105.7	−108.2	−118.3
H2SiSO	102.1	106.1	121.7
H3SSiO	3.4	−1.4	63.2
H4OSiS	111.7	116.3	54.9
	Total Energies (hartrees)[b]		
HF/6-31G*	−763.626 17	−763.598 00	−763.682 39
MP2/6-31G*[c]	−764.009 31	−763.994 22	−764.059 10
MP3/6-31G*[c]	−764.034 07	−764.015 74	−764.085 37

[a] HF/6-31G* structures in angstroms and degrees. For the numberings of atoms, see Figure 7. [b] Total energies of reactants are −763.598 04 (HF/6-31G*), −763.979 42 (MP2/6-31G*), and −764.006 72 (MP3/6-31G*). [c] Calculated at the HF/6-31G* structures.

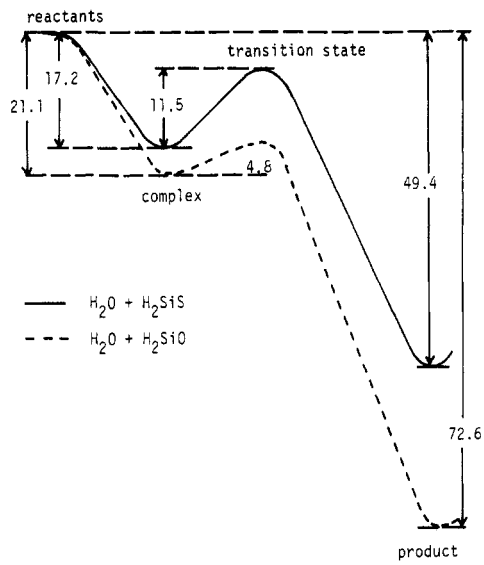

Figure 8. Energy profiles (kcal/mol) at the MP3/6-31G* level for the $H_2O + H_2SiS$ (full line) and $H_2O + H_2SiO$ (dotted line) reactions.

(33) Lias, S. G.; Liebman, J. F.; Levin, R. D. *J. Phys. Chem. Ref. Data* 1984, *13*, 695.

What factors are responsible for the difference in the reactivities of silanethione and silanone? As Figure 4 shows, the frontier orbital π (−10.3 eV) and π^* (0.5 eV) energy levels of silanethione are 2.0 eV higher and 1.0 eV lower, respectively, than the π (−12.3 eV) and π^* (1.5 eV) levels of silanone. If the reactions would be "frontier-controlled", one should see a more facile attack of water on silanethione than on silanone. As seen in Figure 8, this is not the case. Apparently, the lower reactivity of silanethione is due to the fact that the silicon–sulfur double bond is less polarized than the silicon–oxygen double bond.

Despite the less polarized double bond, silanethione is still too reactive to be isolated under normal conditions. In the interest in preparing an isolable silanethione, one should note that the transition state for the $H_2Si{=}S + H_2O$ reaction lies only 5.7 kcal/mol below the reactants, in marked contrast with the energy difference of 16.3 kcal/mol between the reactants and transition state in the $H_2Si{=}O + H_2O$ reaction. This means that the reactivity of silicon–sulfur double bonds can be more easily controlled not only by the steric effect of very bulky substituents but also by the electronic effect of relatively small substituents.[34] Obviously, the electronic effect of small substituents should reduce further the dipolar character in the silicon–sulfur double bond of $H_2Si{=}S$ (and increase the HOMO–LUMO energy gap).

Concluding Remarks

Comparisons with silanone as well as formaldehyde reveal several intriguing aspects of the structural and energetic properties of silanethione in the ground, excited, and protonated states. An important finding is that silicon is much less reluctant to form double bonds with sulfur than with oxygen. Thus, silanethione is more stable and less reactive than silanone. The major obstacle to the successful isolation of silanethione is the relatively high reactivity. In order to design an isolable silanethione, the hydrogen atoms in $H_2Si{=}S$ should be replaced by substituents that deduce the polarity of the silicon–sulfur double bond. A theoretical study along this line is in progress.

Acknowledgment. All calculations were carried out at the Computer Center of the Institute for Molecular Science and at the Computer Center of Tokyo University with the IMSPAK (WF10-8) and GAUSSIAN 80 (WF10-24) programs in IMS Computer Center library program package. We are grateful to Dr. D. A. Dixon for sending a preprint of ref 24 prior to publication.

Registry No. Si, 7440-21-3; S, 7704-34-9; $H_2Si{=}S$, 69639-29-8; H_2O, 7732-18-5; $H_2C{=}O$, 50-00-0; $H_2Si{=}O$, 22755-01-7; HSiSH, 99278-16-7; H_2SiSH^+, 80401-43-0; $HSiSH_2^+$, 101630-69-7; H_2SiOH^+, 66639-72-3; $HSiOH_2^+$, 101630-70-0.

(34) For a theoretical attempt to reduce the reactivity of silicon–carbon double bonds by the electronic effect, see: Nagase, S.; Kudo, T.; Ito, K. In *The Proceedings of the Applied Quantum Chemistry Symposium*; Smith, V. H., et al., Eds.; D. Reidel Publishing: Dordrecht, Netherland, in press.

(35) **Note Added in Proof.** As described in the text, the 1,2-H shifts in $H_2Si{=}S$ and $H_2Si{=}O$ are found, also at the MP2 and MP3 levels of calculation, to proceed via a nonplanar transition state, except that at the MP2 level a planar transition state becomes slightly more favorable for the 1,2-H shift in $H_2Si{=}O$.

Titanium-Catalyzed Cycloaddition–Cycloreversion Cascade in the Reaction of Norbornadiene with Bis(trimethylsilyl)acetylene

Karel Mach,* František Tureček, Helena Antropiusová, and Vladimír Hanuš

J. Heyrovský Institute of Physical Chemistry and Electrochemistry, Czechoslovak Academy of Sciences, 121 38 Prague 2, Czechoslovakia

Received September 11, 1985

The $TiCl_4$–Et_2AlCl catalyst induces endo-[2 + 2] cycloaddition of bis(trimethylsilyl)acetylene to norbornadiene. At 20 °C the adduct undergoes a catalyzed Cope rearrangement followed by disrotary ring opening which yields 2,3-bis(trimethylsilyl)-*cis*-bicyclo[4.3.0]nona-2,4,8-triene as a single low molecular weight product. At elevated temperatures the Cope rearrangement is followed by a 1,3-sigmatropic shift and ring opening, yielding isomeric 3,4-bis(trimethylsilyl)-*cis*-bicyclo[4.3.0]nona-2,4,8-triene. The $TiCl_4$–Et_2AlCl system also catalyzes the Diels–Alder addition of bis(trimethylsilyl)acetylene to either 1:1 adduct, affording a single tricyclic triene, 8,9,10,11-tetrakis(trimethylsilyl)tricyclo[5.2.2.$0^{2,6}$]undeca-3,8,10-triene. The latter can be used for a facile preparation of 1,2,4,5-tetrakis(trimethylsilyl)benzene. The reaction mechanism and the products of the catalyst deactivation are discussed.

Introduction

The homogeneous Ziegler–Natta catalysts, derived either from (arene)titanium(II) complexes or from $TiCl_4$ combined with an excess of Et_2AlCl, have recently been shown to induce [6 + 2] cycloadditions of 1,3,5-cycloheptatriene to various trienophiles,[1,2] as well as [4 + 2] cycloadditions of conjugated dienes to bis(trimethylsilyl)acetylene (BTMSA).[3] The $TiCl_4$–Et_2AlCl catalyst proved to be especially active in inducing cross-additions of unsaturated substrates, and we were encouraged by its catalytic properties to explore the reaction of BTMSA with the highly reactive bicyclo[2.2.1]hepta-2,5-diene (norbornadiene, NBD). Of special interest was the mode of the NBD addition, since in the reaction with 1,3,5-cycloheptatriene we obtained products of both the [2 + 2 + 2] and the [6 + 2] addition.[2] In the transition-metal-catalyzed cycloaddition

(1) Mach, K.; Antropiusová, H.; Tureček, F.; Hanuš, V.; Sedmera, P. *Tetrahedron Lett.* **1980**, *21*, 4879. Tureček, F.; Hanuš, V.; Sedmera, P.; Antropiusová, H.; Mach, K. *Collect. Czech. Chem. Commun.* **1981**, *46*, 1474.

(2) Mach, K.; Antropiusová, , H.; Hanuš, V.; Sedmera, P.; Tureček, F. *J. Chem. Soc., Chem. Commun.* **1983**, 805. Mach, K.; Antropiusová, H.; Petrusová, L.; Hanuš, V.; Tureček, F.; Sedmera, P. *Tetrahedron* **1984**, *40*, 3295.

(3) Mach, K.; Antropiusová, H.; Petrusová, L.; Tureček, F.; Hanuš, V.; Sedmera, P.; Schraml, J. *J. Organomet. Chem.* **1985**, *289*, 331.

0276-7333/86/2305-1215$01.50/0